

## Ultrasonographic optic nerve sheath diameter technical pitfalls and imaging artifacts

Mohammad I. Hirzallah, Aarti Sarwal, Aaron M. Dentinger, Chiara Robba, Jurgita Valaikienė, Piergiorgio Lochner, Felix Schlachetzki, David M. Mills, Michael Ertl, Ryan Hakimi, Shreya Bhise, Jakob Pansell

### Angaben zur Veröffentlichung / Publication details:

Hirzallah, Mohammad I., Aarti Sarwal, Aaron M. Dentinger, Chiara Robba, Jurgita Valaikienė, Piergiorgio Lochner, Felix Schlachetzki, et al. 2025. "Ultrasonographic optic nerve sheath diameter technical pitfalls and imaging artifacts." *Journal of Ultrasound in Medicine* 44 (6): 1106–20. <https://doi.org/10.1002/jum.16655>.



# Ultrasonographic Optic Nerve Sheath Diameter Technical Pitfalls and Imaging Artifacts

Mohammad I. Hirzallah, MD, MMSc , Aarti Sarwal, MD, FAAN, FNCS, FCCM, RPNI, Aaron M. Dentinger, PhD, Chiara Robba, MD, PhD, Jurgita Valaikienė, MD, PhD , Piergiorgio Lochner, MD, PhD, Felix Schlachetzki, MD , David M. Mills, PhD, Michael Ertl, MD, Ryan Hakimi, DO, MS, NVS, RPNI, CPB, FNCS, FCCM, FAAN, Shreya Bhise, MD, MBA, Jakob Pansell, PhD

Received November 5, 2024, from the Departments of Neurology and Neurosurgery, Baylor College of Medicine, Houston, Texas, USA (M.I.H.); Center for Space Medicine, Baylor College of Medicine, Houston, Texas, USA (M.I.H.); Department of Neurology, Virginia Commonwealth University School of Medicine, Richmond, Virginia, USA (A.S.); GE HealthCare, Technology & Innovation Center, Niskayuna, New York, USA (A.M.D., D.M.M.); IRCCS Policlinico San Martino, Genova, Italy (C.R.); Clinic of Neurology and Neurosurgery, Institute of Clinical Medicine, Faculty of Medicine, Vilnius University, Vilnius, Lithuania (J.V.); Department of Neurology, Saarland University Medical Center, Homburg, Germany (J.V., P.L.); Department of Neurology, University of Regensburg, Center for Vascular Neurology and Intensive Care, Regensburg, Germany (F.S.); Department of Neurology and Clinical Neurophysiology, University of Augsburg, Augsburg, Germany (M.E.); Department of Medicine (Neurology), University of South Carolina School of Medicine-Greenville, Greenville, South Carolina, USA (R.H.); President-Elect, American Society of Neuroimaging, Spartanburg, South Carolina, USA (R.H.); GE HealthCare Point of Care & Handheld, Milwaukee, Wisconsin, USA (S.B.); Department of Clinical Neuroscience, Karolinska Institute, Stockholm, Sweden (J.P.); and Department of Anesthesia and Intensive Care, Karolinska University Hospital, Stockholm, Sweden (J.P.). Manuscript accepted for publication January 18, 2025.

The project described within was funded in part with federal funds from the U.S. Department of Health and Human Services (HHS); Administration for Strategic Preparedness and Response (ASPR); Biomedical Advanced Research and Development Authority (BARDA), under contract number 75AS0123C00035. The contract and federal funding are not an endorsement of the study results, product or company.

Address correspondence to Mohammad I. Hirzallah, Departments of Neurology and Neurosurgery, Baylor College of Medicine, Houston, TX, USA.

E-mail: mohammad.hirzallah@bcm.edu

## Abbreviations

ALARA, as low as reasonably achievable; ONSDext, external ONSD; ONSDint, internal ONSD; ICP, Intracranial pressure; MI, mechanical index; ONSD POCUS QCC, ONSD point-of-care ultrasonography quality criteria checklist; ONS, optic nerve sheath; ONSD, optic nerve sheath diameter; SHB, striped hyperechoic band; TI, thermal index

Ultrasonographic optic nerve sheath diameter (ONSD) is a non-invasive intracranial pressure (ICP) surrogate. This article discusses the effect of ultrasound settings and imaging artifacts on ONSD assessment. Ultrasound settings that may affect ONSD assessment include gain, dynamic range, frequency, harmonic imaging, and focal zones. Artifacts can be related to imaged structures (acoustic shadowing, enhancement, comet tail, and speckle artifacts) or to beam properties (partial volume and refraction artifacts). In addition, optic nerve sheath (ONS) properties such as echogenicity changes based on ICP or ONS kinking are discussed.

**Key Words**—artifacts; intracranial pressure; noninvasive; optic nerve sheath diameter; ultrasound; ultrasound physics

Intracranial pressure (ICP) assessment is essential for the management of severe acute brain injury. While invasive ICP monitoring remains the gold standard, optimizing non-invasive ICP assessment methods would improve patient care when invasive ICP monitoring is not available or contraindicated.<sup>1</sup> Ultrasonographic optic nerve sheath diameter (ONSD) is a non-invasive ICP surrogate, that takes advantage of the continuity of the subarachnoid space surrounding the optic nerve to the basal cisterns. However, the small size of the optic nerve sheath (ONS) and the surrounding structures introduces technical challenges for its measurement using current ultrasound probes including sensitivity to variations in imaging and measurement technique, susceptibility to artifacts, and technical challenges.<sup>2</sup> This variability may be in part due to a limited understanding of ultrasound device settings and imaging artifacts in ONSD measurement which may lead to under or overestimating the measurement. While the effect of technical challenges and artifacts in B-mode ultrasonography is well-documented in other ultrasound imaging applications,<sup>3,4</sup> these challenges are not completely described in the case of ONSD ultrasonography. A recent consensus statement, the ONSD point-of-care ultrasonography quality criteria checklist (ONSD POCUS QCC) recommends careful evaluation and exclusion of artifacts prior to ONSD measurement.<sup>5</sup> This article aims to provide a classification and visual guide to the effects of ultrasound settings and artifacts on ONSD imaging and measurement.

This classification will be accompanied by an explanation of the underlying ultrasound physics, device limitations, anatomic considerations, and troubleshooting recommendations.

## Standard ONSD View

A standard ONSD ultrasonography view consists of a lateral axial image (with sagittal views being acceptable) obtained by placing a linear ultrasound probe imaging at a frequency of  $\geq 7.5$  MHz on the closed upper eyelid. An ocular or ophthalmic preset should be used when available with emphasis on avoiding eye pressure, adhering to as low as reasonably achievable (ALARA) principle, including reducing scan times and acoustic power. The mechanical index (MI) should be  $\leq 0.23$  and thermal index (TI)  $\leq 1$  per US FDA guidelines for ophthalmic imaging.<sup>6</sup> Body position can affect measurement and should be standardized. Optimizing probe positioning, B-mode gain, dynamic range, and focus position will aid in obtaining the image with the clearest anatomic differentiation which should be used for measurement. While current recommendations are to use internal ONSD (ONSDint) in clinical practice and both ONSDint and external ONSD (ONSDext) for research,<sup>5</sup> this is an evolving area of research.<sup>7</sup> However, it is important to understand, that ONSDint vs ONSDext are different measurements<sup>8</sup> and inconsistency in using them would lead to misdiagnosis.<sup>5</sup> A recent consensus provided a number of statements aiming to standardize the ONSD measurement.<sup>5</sup> Figure 1 represents a “standard” ONSD image and measurement based on current ONSD POCUS QCC recommendations.

## Effect of Ultrasound Device Settings on ONSD Measurement

### *Ultrasound Power and Gain*

Ultrasound power relates to the transmitted ultrasound energy from the ultrasound probe, this is usually limited in ophthalmic presets to maintain an MI  $\leq 0.23$ .<sup>6</sup> Gain is a post-processing feature that amplifies the received ultrasound signal. Therefore, increasing gain does not increase ultrasound power

transmitted to the patient. Near and far gain adjustments allow differential adjustment of the gain in the top or bottom half of the image. In addition, gain adjustments can also be performed post image acquisition. It is important to adjust the ultrasound gain levels to be able to view the boundaries of the ONS and perform the measurement correctly. Undergaining an image would degrade the image by reducing ultrasound signals from less echoic structures below detectable gray levels on the display. Overgaining an image would degrade the image by increasing reflections from hyperechoic structures and thus obscuring the contrast from different structures<sup>9</sup> (Figure 2).

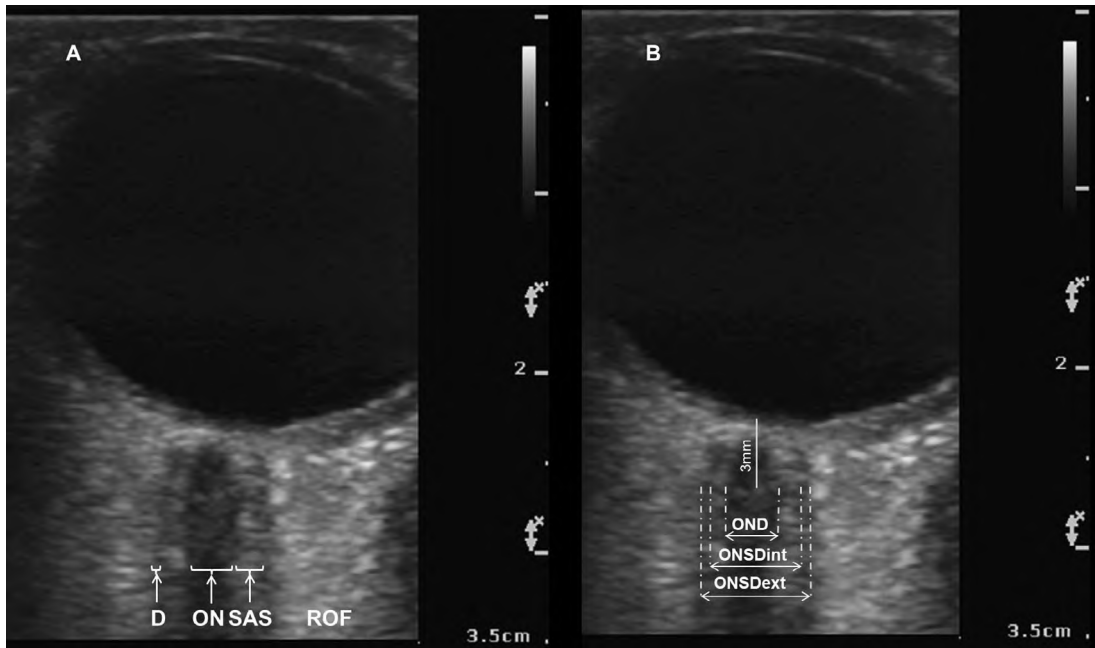
### *Dynamic Range*

Dynamic range represents the ratio between the darkest and brightest signal mapped to the grayscale levels. Adjusting the dynamic range can improve the contrast between different structures. A higher dynamic range leads to a wider range of ultrasound signal levels mapped to the gray scale visible on the display and may affect discrimination of ONSD layers by decreasing the contrast of the margins. Narrow dynamic range reduces the range of grayscale displayed resulting in higher contrast with more black and white structures and creates better discrimination amongst the gray structures but may not allow visualization of structures with thin layers (Figure 3).<sup>10</sup> The dynamic range setting thereby affects the ability to distinguish the structures of the ONS and can be used to optimize images. While the effect of different dynamic range values on ONSD measurement was not directly evaluated, it has been shown to significantly change measurement of anatomic structures such as the carotid intima media thickness.<sup>11</sup>

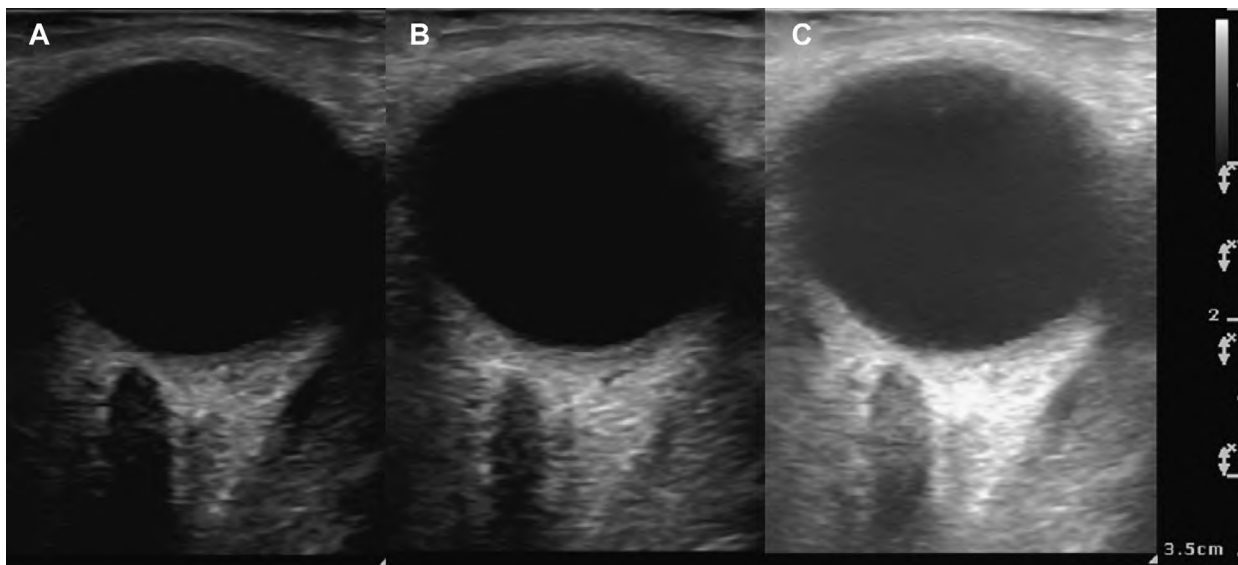
### *Image Resolution*

Image resolution is affected by several factors controllable by the ultrasound operator and factors dependent on the technical specifications of the ultrasound device. The ultrasound operator can improve resolution by changing the imaging mode, increasing frequency, and adjusting focal zones when permissible by the ultrasound device. These considerations will be discussed in the following sections. Factors related to technical specification include probe frequency, aperture, and bandwidth along with image enhancement

**Figure 1.** Standard ONS view. **A**, Anatomic structures. **B**, Different measurements performed at 3 mm depth. D, dura; ON, optic nerve; OND, optic nerve diameter; ONSDint, internal ONSD; ONSDext, external ONSD; ROF, retro-orbital fat; SAS, subarachnoid space. Images were obtained using a Philips Sparq machine and an L12-4 linear array transducer with a frequency range of 4 to 12 MHz and 37 mm footprint.



**Figure 2.** Effect of gain adjustment on ONSD ultrasonography. **A**, Under-gained images appear too dark and darker (hypoechoic) structures may be difficult to visualize, the gain in this image was 31%. **B**, When gain is adjusted properly, different structures and their boundaries can be differentiated, the gain in this image was 55%. **C**, Over-gained images may result in brighter structures obscuring darker structures, the gain in this image was 92%. Images were obtained using a Philips Sparq machine and an L12-4 linear array transducer with a frequency range of 4 to 12 MHz and 37 mm footprint.



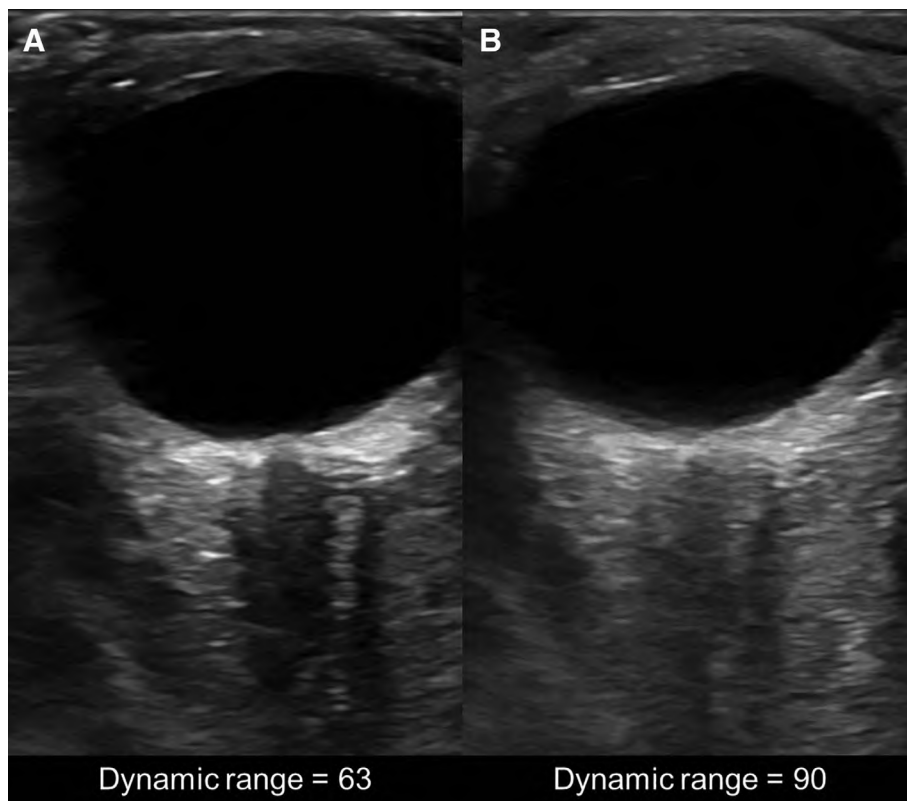
techniques including acquisitions modes (such as spatial compounding) and post processing algorithms. Aperture refers to the width of the transducer that, along with the wavelength, determines the imaging beam width,<sup>12</sup> to improve spatial resolution, modern ultrasound probes have increased the number of piezoelectric crystals receiving the returning beam based on return time. This is referred to as dynamic aperture<sup>13</sup> and is most impactful in near field applications like ophthalmic imaging. Post processing could be used to enhance edges and increase contrast in the images. Edge enhancement typically uses filters to increase the higher spatial frequencies in the image but need to balance the increase in noise in the filtered image. Improved contrast may be achieved with speckle reduction filters that attempt to smooth the image while preserving edges. Spatial compounding is another linear probe imaging mode that reduces speckle and improves the contrast of

structures. This is done by steering ultrasound beams in multiple different directions and combining the images which reduces speckle artifacts from non-orthogonal reflections.<sup>13</sup>

#### *Ultrasound Frequency, Probe Selection, and Imaging Modes*

The association between frequency and resolution is a well-known fact of ultrasound physics, caused by the wavelength limiting the size of structures that can be reliably distinguished.<sup>10,14</sup> In ONSD ultrasonography, it has been shown both in theoretical calculations and experimental simulation that the lateral resolution is  $\sim 0.5$  mm with a 10 MHz probe and 0.6 mm with a 6 MHz probe,<sup>15</sup> which should be enough to distinguish the ONS subarachnoid space (1-mm thick on average) and dura (0.7-mm thick on average).<sup>7</sup> ONSD imaging should start with selecting

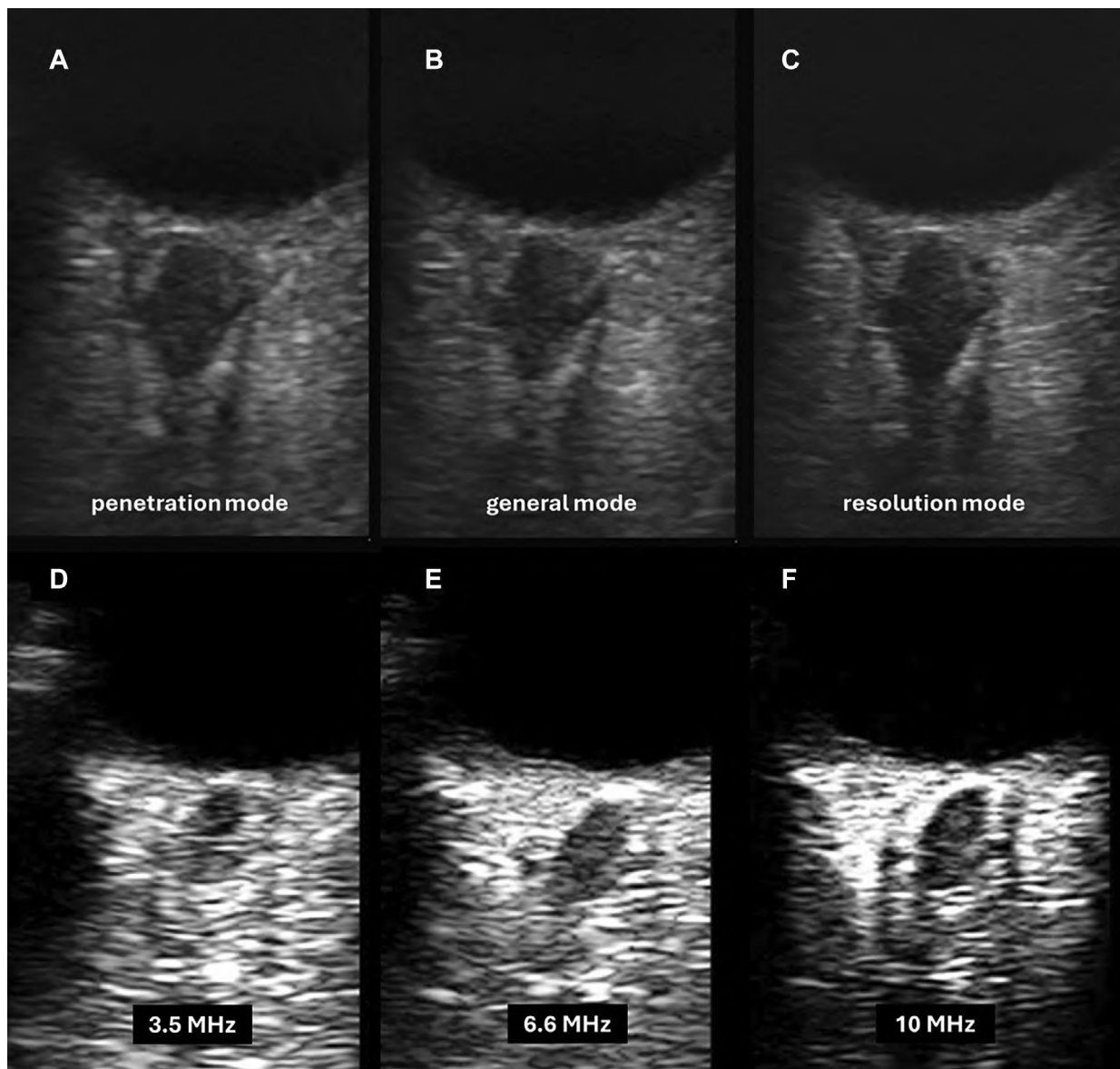
**Figure 3.** The effects of dynamic range on image quality. **A**, Lower dynamic range improves the visualization of boundaries at the expense of some loss of smaller details; **B**, Higher dynamic range leads to loss of contrast between boundaries but may improve visualization of finer details. Images were obtained using a GE Vivid S70 machine and an 11 L-D linear transducer with a frequency range of 4.5 to 12 MHz and 47 mm footprint.



a probe with a suitable frequency range. Ultrasound probes are designed to operate over a range of frequencies with the center frequency provided by the system as a default or selected by the user. Some

diagnostic ultrasound machines allow for frequency adjustment within the probe frequency range whereas other machines allow for the choice of pre-determined presets including penetration, general,

**Figure 4.** Effect of ultrasound frequency and modes on ONSD assessment. Notice the smaller speckle size and sharper edges with higher resolution. **A**, Penetration mode uses the lower end of the resolution range to improve imaging deeper structures. **B**, General mode uses the middle of the probe's frequency range. **C**, Resolution mode uses the higher end of the frequency range for improved resolution. Some diagnostic ultrasound machines allow for frequency adjustment within the probe frequency range. The figure shows examples of such scans obtained with **(D)** 3.5 MHz, **(E)** 6.6 MHz, and **(F)** 10 MHz frequencies. **(A–C)** Images were obtained using a Philips Sparq machine and an L12-4 linear array transducer with a frequency range of 4 to 12 MHz and 37 mm footprint. **(D–F)** Images were obtained using an Esaote Biosound MyLab 25 machine and an Esaote LA332 linear array transducer with a frequency range of 3 to 10 MHz and 33 mm footprint.



and resolution modes. Penetration mode uses the lower end of the frequency range to prioritize imaging deeper structures over image resolution while resolution mode uses the higher end of the frequency range to prioritize higher resolution of superficial structures. General mode is usually in the middle of that frequency range (Figure 4). Resolution and general modes may perform better with ONSD imaging due to higher frequency than penetration mode. However, there is no set rule for which mode to use and the examiner should adjust the modes as needed to improve image quality.

### ***Tissue Harmonic Imaging***

Tissue harmonic imaging, also known as pulse inversion or second harmonic imaging, takes advantage of the distortion of the speed of ultrasound beams through a medium which results in returning

echoes at the transmitted (fundamental) frequency and weaker echoes at integral multiples of transmitted frequency called harmonics. The second harmonic with a frequency of twice the fundamental frequency can be useful but the third order and higher harmonics are highly absorbed by tissue because of their high frequency limiting their ability to travel back to the probe. Harmonic frequencies are less distorted by tissues than the fundamental frequency because they arise from deeper tissues and are not distorted by superficial tissues. Therefore, harmonic imaging can have better clarity than fundamental imaging. The ultrasound machine performs harmonic imaging by blocking the returning fundamental frequency and only receiving the harmonic frequencies. A limitation of harmonic imaging is the low amplitude of harmonic which may cause low dynamic range and a poor signal-to-noise

**Figure 5.** Effect of harmonic imaging on image quality. **A**, ONSD image using resolution mode. In comparison, **(B)** is the same image after switching to harmonic resolution mode. While some boundaries appear clearer, the overall dynamic range is lower, and the image appears darker. Images were obtained using a Philips Sparq machine and an L12-4 linear array transducer with a frequency range of 4 to 12 MHz and 37 mm footprint.

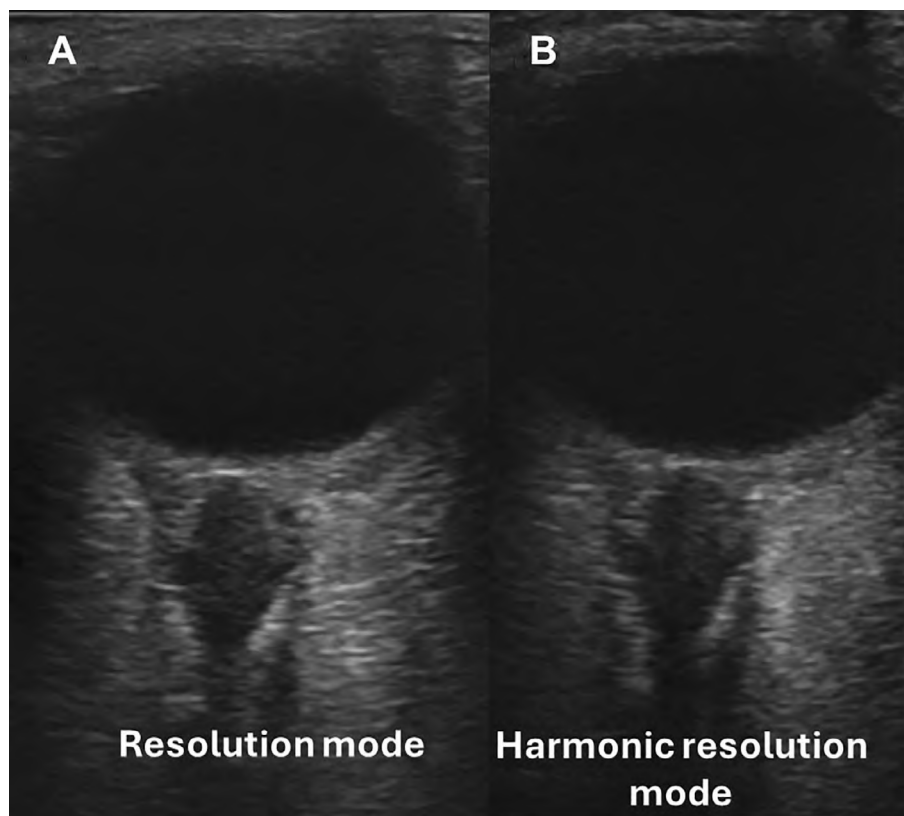
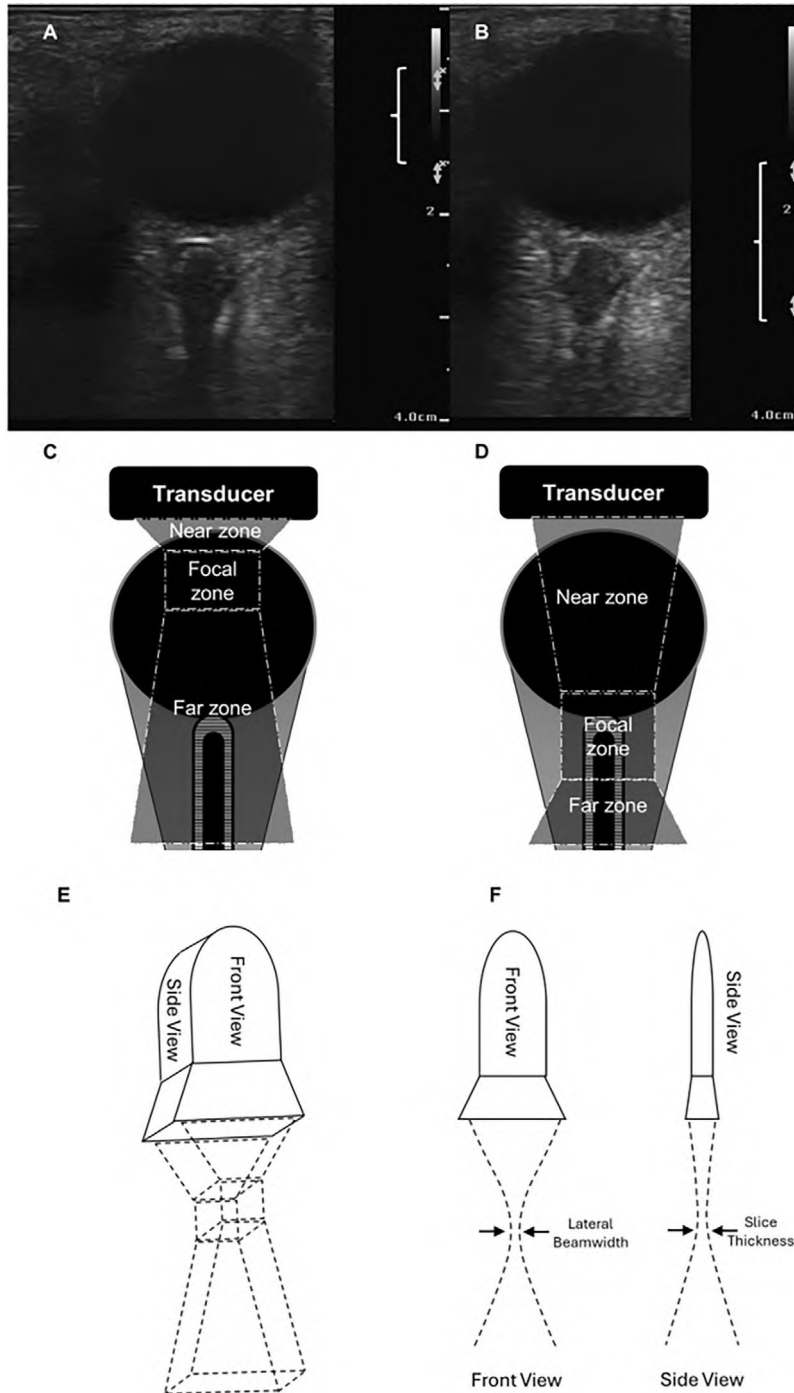


**Figure 6.** Effect of adjusting the focal zone on ONSD assessment. **A**, Demonstrated the focal zone adjusted to the top of the frame as labeled by the open bracket while **(B)** demonstrated the focal zone adjusted to the bottom of the frame, **(C and D)** are illustrations of the focal zone adjustments. **E**, Ultrasound beam is 3-dimensional and so are its focal zones, **(F)** The front face of the beam determines lateral resolution whereas the side face determines slice thickness. Images were obtained using a Philips Sparq and an L12-4 linear array transducer with frequency range of 4 to 12 MHz.



ratio. Overall, harmonic imaging can improve image clarity at the expense of dynamic range and signal power resulting in darker images.<sup>13</sup> In the example provided in Figure 5 demonstrates the effect of harmonic imaging on ONSD assessment.

### Focal Zone

Transmitted ultrasound beams have a similar width to the probe face in the near zone, before narrowing down to the minimal width at the focal zone and widening again in the far zone, resembling an hourglass shape (Figure 6). While each transducer has its own “natural” focal zone, electronic beamforming allows for additional control of the transmit focusing, including enabling multiple focal zones at different depths with the trade off in a reduction in the frame rate. The focal zone represents the zone with the highest lateral resolution allowing for the best discrimination of anatomic structures.<sup>10</sup> Some ultrasound devices allow adjustment of the location of the focal zone. Adjusting the focal zone to the level of the optic nerve head is important to improve lateral resolution and reduce imaging artifacts. In addition to the focal zone of the transmitted ultrasound beam, the focal zone of the received ultrasound beam is important for determining lateral resolution. Modern ultrasound systems allow for several successive transmit beams focused at different depths that are spliced into a single image. The result is an optimally focused image over a larger range of depths.

## Effects of ONS Properties on Image Features

### Change in ONS Attenuation Based on ICP

An observation noted by multiple experts is a more hypoechoic ONS in some cases of elevated ICP.<sup>5</sup> This may be due to increased CSF in the ONS subarachnoid space. However, as shown in Figure 7, not all cases of ONS distention are associated with a hypoechoic ONS. One study called this phenomenon of hypoechoic ONS “cystic ONS” and noted that 80% of patients with elevated ICP had hypoechoic ONS and 12.5% of patients with normal ICP had hypoechoic ONS.<sup>16</sup> An additional consideration is that inter-individual variation in the density of trabecular meshwork may contribute to this phenomenon even in the absence of elevated ICP<sup>17</sup> (the trabecular meshwork also plays a role in the effect of gaze direction discussed below). A formal measurement method of ONS hypoattenuation is not currently available. Muscle ultrasound literature has explored echogenicity measurements, but these are not currently available on commercial ultrasound systems.<sup>18</sup> Echogenicity can also be measured post hoc using computer software but there is lack of a gold standard calibration to define grayscale across different machines and these measurements are sensitive to the gain settings.<sup>19</sup> Echogenicity assessment techniques may prove useful for ONS assessment in the future. Meanwhile, it is important to be aware of ONS echogenicity changes to avoid missing its boundaries while measuring ONSD and have a higher suspicion of elevated ICP in the presence of a hypoechoic ONS.

**Figure 7.** The effect of elevated ICP on ONSD echogenicity. All three panels show ONSD >6 mm. However, panels (A) and (B) show a darker, more hypoattenuating sheath, than (C). Images were obtained using a Philips Sparq machine and an L12-4 linear array transducer with a frequency range of 4 to 12 MHz and 37 mm footprint.

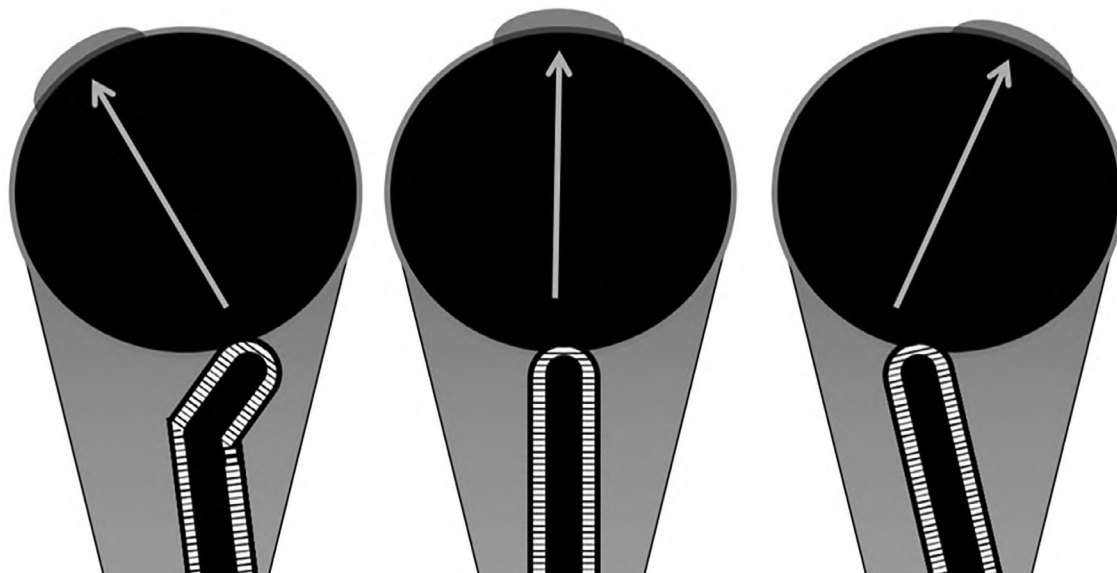
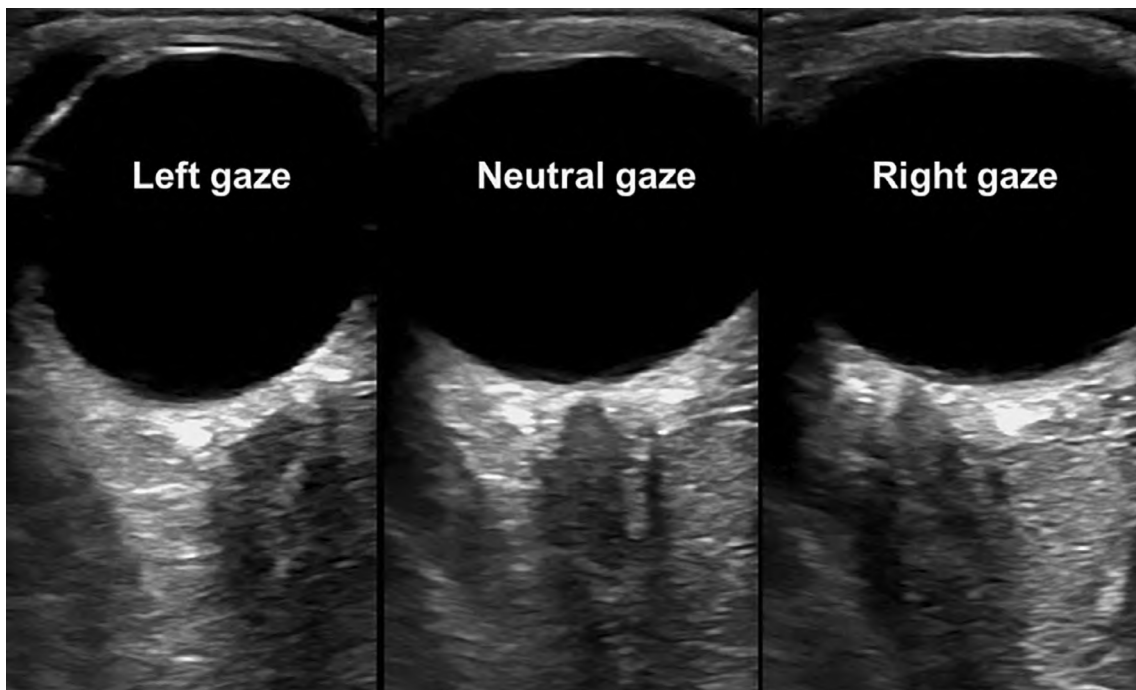


**Anisotropy, Insonation Angle, and Gaze Direction**

Best practices for ONSD imaging include neutral gaze direction and aligning the imaging axis with optic nerve (ON) axis.<sup>5</sup> To understand the importance of

these considerations, it is important to understand the structure of the ON and ONS, the effect of gaze direction on these structures and anisotropy artifacts. The ONS subarachnoid space contains a complex

**Figure 8.** Images obtained from the same subject in the same scanning session with different gaze directions. Notice the effect of gaze direction on the ONS appearance and size. Arrows represent gaze direction in the illustration. Images were obtained using a GE Vivid S70 machine and an 11 L-D linear transducer with a frequency range of 4.5 to 12 MHz and 47 mm footprint.



structure of trabeculae, septa, and pillars that project radially from the nerve.<sup>17</sup> This likely contributes to characteristic striped hyperechoic band (SHB) of the subarachnoid space<sup>20</sup> and to studies imaging the ONS ex vivo in the lateral direction having an inverse appearance where the subarachnoid space and optic nerve are both hyperechoic and difficult to distinguish.<sup>21</sup> Additionally, gaze direction can change ONSD values by deforming the ONS.<sup>22,23</sup> Finally, it is important to understand the effects of fiber direction on ultrasound attenuation, known as anisotropy. Anisotropy is commonly described in muscle tissue due to its directional fiber bundles, which results in changing ultrasound attenuation based on the angle of the sound beams (angle of insonation) in relation to the fibers. The maximum returned echoes are seen when the ultrasound beams are perpendicular to the muscle fibers resulting in hyperechoic appearance, whereas when the angle is reduced and the beams are parallel to muscle fibers, they will appear hypoechoic resembling vascular structures.<sup>12</sup> Anisotropy may describe why the ON is typically hypoechoic in clinical practice and in-vivo studies where the insonation

angle is parallel to the ON but bright in ex-vivo studies where nerve specimens are insonated at a right angle.<sup>21</sup> Figure 8 demonstrates the effect of gaze direction, insonation angle, and anisotropy on ONSD measurements and image quality.

## Ultrasound Artifacts

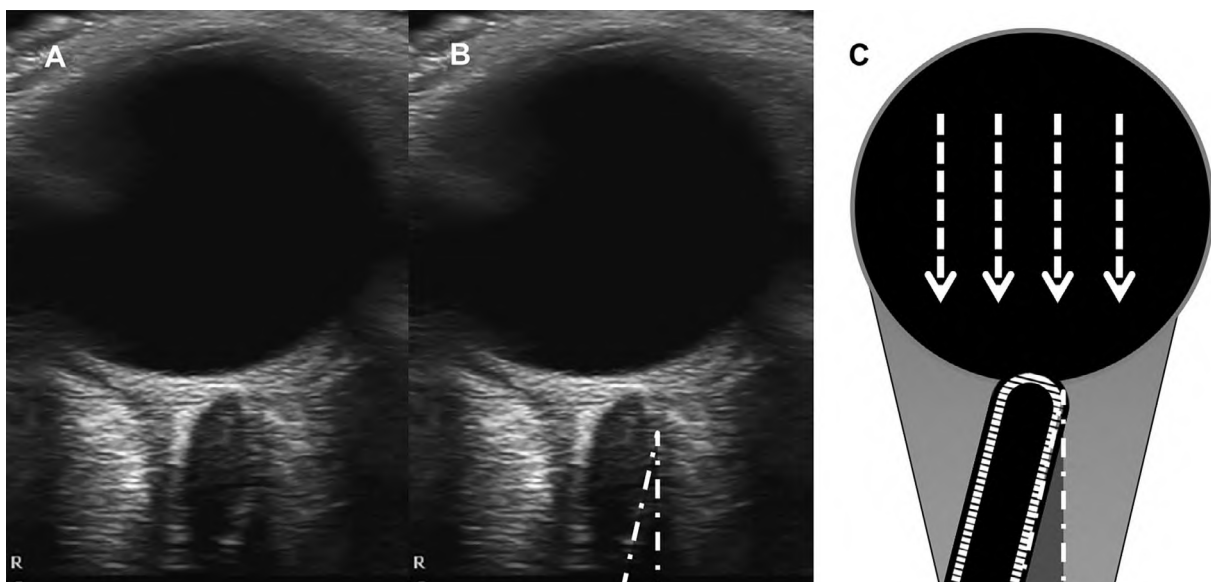
Ultrasound artifacts relevant to ONS imaging can include those primarily related to imaged structures and those related to ultrasound beam properties and interpretation. Artifacts related to imaged structures include shadowing, enhancement, comet tail, and speckle artifacts. Artifacts related to ultrasound beam properties and image processing include beam width, refraction, range ambiguity, and speed error artifacts.<sup>3</sup>

### *Ultrasound Artifacts Related to Imaged Structure*

#### *Acoustic Shadowing Artifacts*

Shadowing artifacts appear as a hypoechoic shadow obscuring the ONS boundaries which may affect measurement accuracy. This happens when the

**Figure 9.** Illustration of ONSD shadow artifacts. **A**, ONSD image with shadow artifacts; **B**, Boundaries of the shadow artifact are highlighted by a striped line; **C**, Diagram illustrating the mechanism of a shadow artifact; as the ultrasound beams encounter a strongly attenuating structure, in this case, the ONS imaged at angle, the ultrasound waves are not transmitted distally, resulting in ultrasound signal loss and an acoustic shadow on the display. The striped arrows represent the direction of the ultrasound beam and the triangle with the striped boundaries represents a shadow artifact. Images were obtained using a Philips Sparq and an L12-4 linear array transducer with a frequency range of 4 to 12 MHz and 37 mm footprint.



ultrasound beam path contains strongly attenuating or reflecting structures like the optic disk, an off-axis optic nerve, or drusen attenuating the ultrasound signal resulting in loss of signal distally and creating a shadow distal to that structure on the display.<sup>3</sup> Troubleshooting consists of small adjustments to avoid structures casting the shadow and avoid imaging axis and ON misalignment as imaging the ON at an angle can lead to shadowing this is likely due to the trabeculae, septa, and pillars that are oriented at a right angle relative to nerve axis<sup>24</sup> having different acoustic properties when imaged at an angle as discussed earlier (Figure 9).

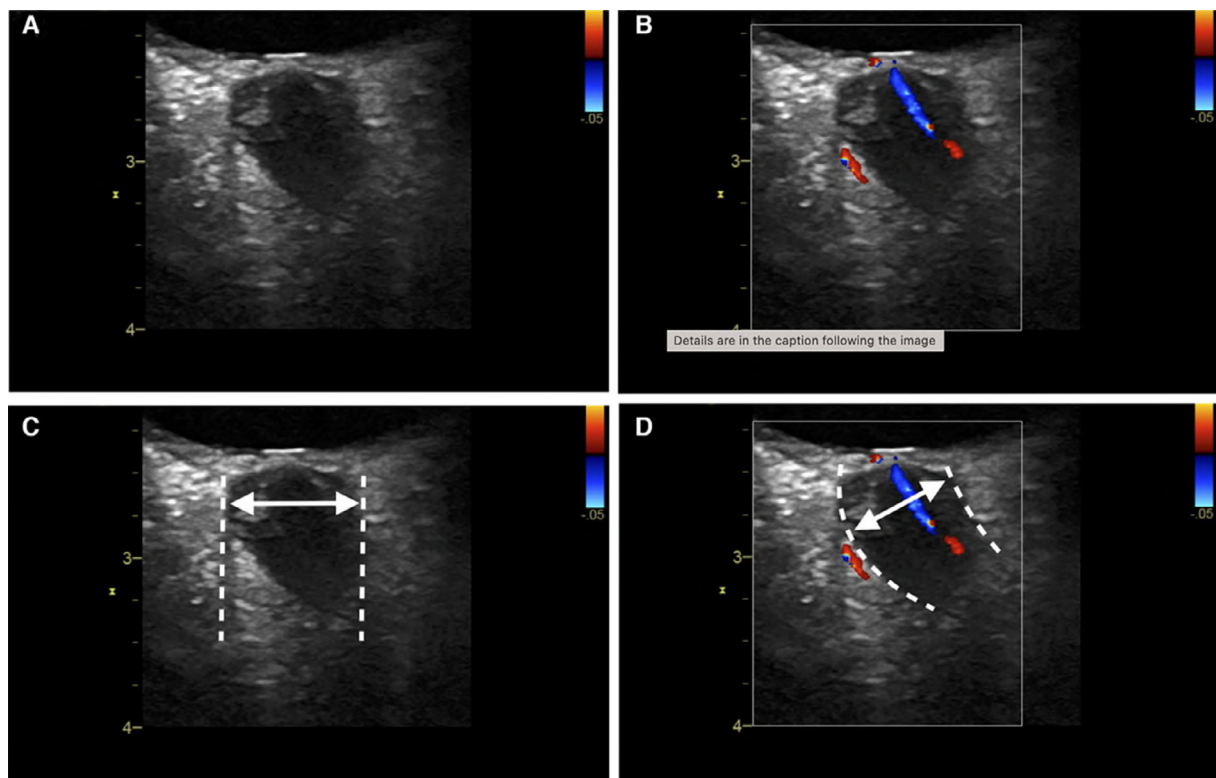
Color Doppler of the central retinal artery and/or vein has been suggested as an aid in identifying the proper direction of the ON and in centering the measurement correctly (Figure 10). In theory, this may help

avoid measurement of shadow artifacts.<sup>25</sup> A protocol using this technique has been validated with an excellent inter-rater reliability.<sup>26</sup> However, this technique has not been directly compared to an approach without color Doppler and that the examiner should maintain an MI  $\leq 0.23$  and TI  $< 1$  after switching to color Doppler since it increases acoustic power which may result increasing MI and TI.<sup>10</sup>

#### Enhancement Artifacts

Enhancement artifacts occur when ultrasound beam path crosses a weakly attenuating structure such as the eye vitreous fluid. This leads to a higher ultrasound signal amplitude compared to surrounding tissues resulting in brighter structures distal to the weakly attenuating tissues. In this case, a brighter ON and ONS appear distal

**Figure 10.** Using color Doppler to identify ON direction when ONS is obscured by shadow artifact. **A**, Image of the ONSD with a shadow artifact from the edges of the lamina cribrosa on the left side of the optic nerve, potentially giving the impression that the direction of the optic nerve is vertical in the image; **B**, Addition of color Doppler to the same image clarifies the true direction of the optic nerve; **C**, Faulty measurement of ONSDext on the shadow artifact, yielding an ONSDext of 7.3 mm, **D**, Measurement of ONSDext when the true direction of the optic nerve is identified yields an ONSDext of 6.4 mm. Image previously published by Pansell et al.<sup>26</sup> Reproduced under the Creative Commons License CC BY-NC 4.0. Images were obtained using a Vivid S70 machine and an 11 L-D linear transducer with a frequency range of 4.5 to 12 MHz and 47 mm footprint.



to the eye. This artifact usually works to the examiner's advantage. If needed, decreasing the far gain can reduce posterior enhancement and help delineate the boundaries of ONSD. However, it is also sensitive to the angle of insonation<sup>3,4</sup> (Figure 11).

#### Comet Tail Artifact

Comet tail (also known as ring-down or complex reverberation) artifact, is caused by two or more closely spaced reflectors that result in multiple echoes. These multiple echoes are interpreted by the

**Figure 11.** Example of enhancement artifacts in ONSD imaging. **A**, ONSD image with enhancement artifacts; **B**, Area affected by the enhancement artifact is highlighted by a striped circle; **C**, Diagram illustrating the mechanism of an enhancement artifact; as the ultrasound beam (thick arrows) passes through a weakly attenuating structure, the vitreous fluid in this case, the transmitted beams are weakly attenuated resulting in stronger returned signal (thick dashed arrows) and the surrounding tissue is weakly attenuated resulting in weaker returned signal (thinner dashed lines). Images were obtained using a Philips Sparq, an L12-4 linear array transducer (frequency range: 12–4 MHz), and the included ophthalmic preset.

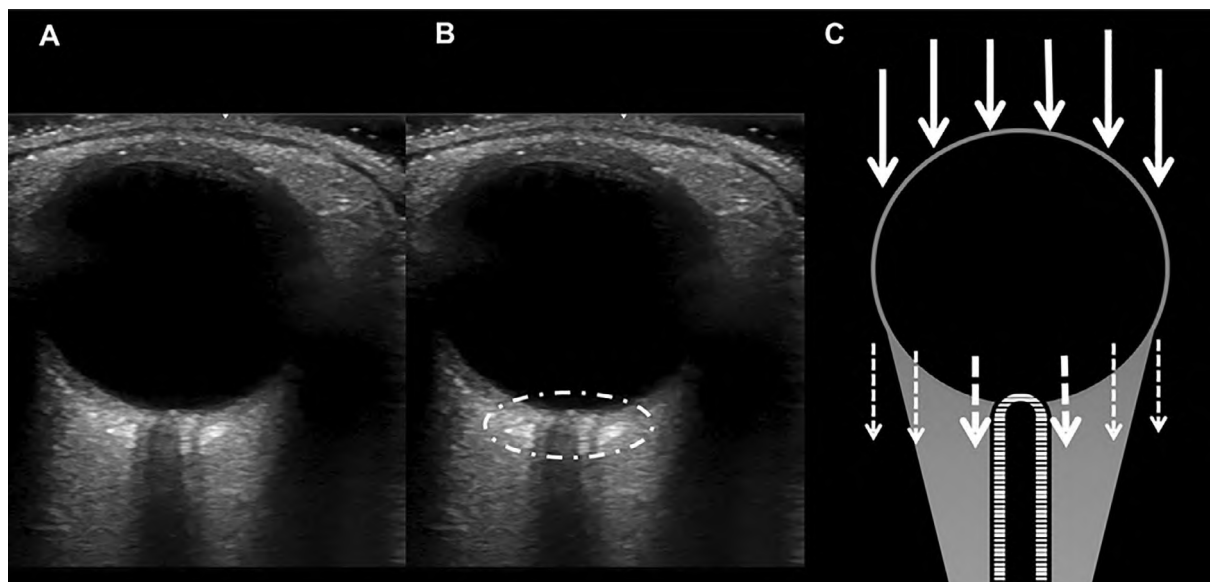
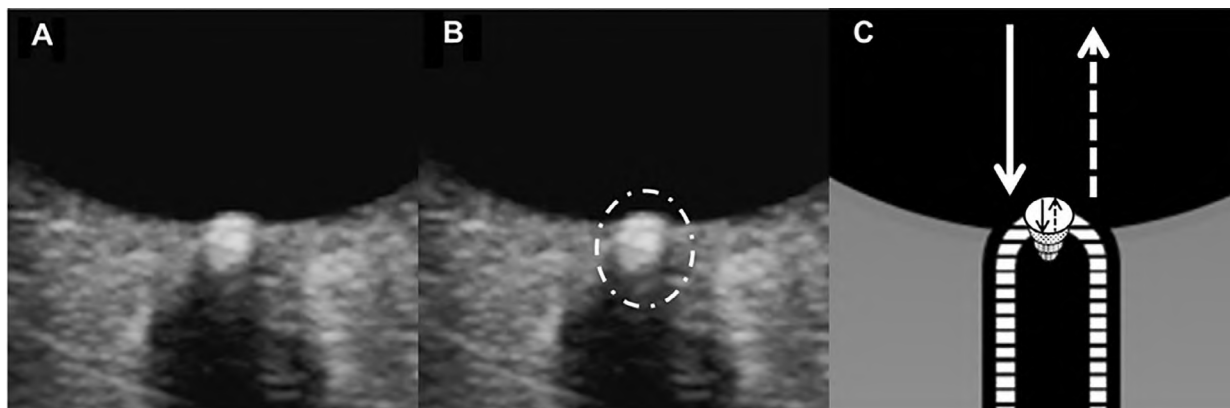


**Figure 12.** Comet tail artifact in ONSD imaging. **A**, an ONSD image with comet tail artifact from optic nerve drusen. **B**, Area affected by the comet tail artifact is highlighted by a striped circle. **C**, Diagram illustrating the mechanism of a comet tail artifact as multiple weaker echoes (represented by dotted circles) resulting in multiple tapered reflections represented by the circles. Images were obtained using a GE LOGIQ E9 machine and an 11 L-D linear transducer with a frequency range of 4.5 to 12 MHz and 47 mm footprint.



ultrasound device as multiple echoes that sequentially move distal to the originating structure with each sequential echo having reduced amplitude. This results in tapered hyperechoic band resembling a comet tail. These artifacts are typically seen deep to calcifications, crystals, or air bubbles.<sup>3,4</sup> When seen at the optic nerve head drusen can appear as a hyperechoic comet tail as shown in Figure 12. Overall, comet tail artifacts are rarely encountered in ONSD imaging.<sup>2</sup>

### Speckle Artifact

Speckle is a property of ultrasound imaging resulting from the scattering of ultrasound beams by closely spaced microstructures that are too small to resolve. This results in increased noise as represented by a granular appearance to some tissue components (Figure 13).<sup>3</sup> Newer imaging technology and post-processing, such as frequency compounding, spatial compounding, and speckle reduction filtering help minimize this artifact.<sup>27</sup> Speckle artifact may contribute to the grainy ONS appearance with unclear boundaries in some cases. However, other artifacts and insonation angles may also contribute to the grainy appearance leading to unclear ONS

boundaries. Therefore, similar troubleshooting steps to other artifacts including changing frequency, insonation angle, and gain may help improve the image.

### Ultrasound Artifacts Related to Beam Properties and Processing

#### Partial Volume Artifacts

Partial volume, also known as slice thickness or beam width artifacts, occurs when an ultrasound beam passes through various structures in the beam width thereby simultaneously sampling tissues with different acoustic properties, causing a “filling-in” effect. This occurs because the ultrasound beam is not a straight line: as the beam exits the transducer it has the same width but narrows down in a focal zone before widening again. The beam also has off-axis low energy beams that may result in additional weaker reflections. In the case of ONSD, an oblique cut sampling both the ON and the ONS simultaneously leads to an elliptical shape of the optic nerve covering a limited depth (Figure 14). This can be avoided by ensuring that the ultrasound imaging axis is aligned with the ON axis, the center of the ultrasound beam with the center of the ON, and the focal zone is

**Figure 13.** Example of the effect of speckle artifact on image quality. **A**, ONSD image with reduced resolution potentially due to speckle artifact; **B**, Area affected by the enhancement artifact is highlighted by a striped circle. **C**, Diagram illustrating the mechanism of a speckle artifact, as the ultrasound beam (thick arrows) are scattered by microstructures (thin dashed arrows), the quality of returned signal (thick dashed arrows) is reduced. Images were obtained using a Philips Sparq and an L12-4 linear array transducer with a frequency range of 4 to 12 MHz and 37 mm footprint.

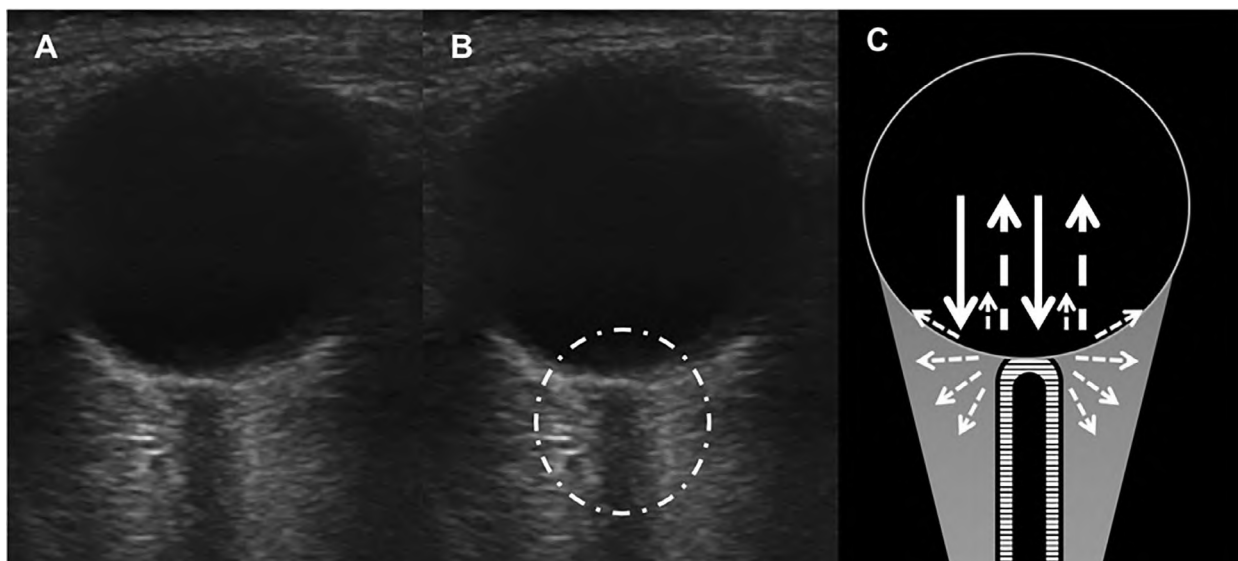


**Figure 14.** Partial volume (volume averaging or slice thickness artifact). **A**, ONSD image with volume averaging due to a misaligned nerve axis and imaging axis, resulting in an off-axis image with sampling of tissues with different acoustic properties, causing a “filling-in” effect; **B**, Area affected by the enhancement artifact is highlighted by a stripped circle; **C**, Diagram illustrating the mechanism of partial volume artifact with and off-axis image, the thick-dashed arrow represents the main beam and the thin curved arrows represent the off-axis low energy beams. **D**, ONSD image with volume averaging due to a kinked optic nerve, resulting in the sampling tissues with different acoustic properties, causing a “filling-in” effect; **E**, Area affected by the enhancement artifact is highlighted by a stripped circle; **F**, Diagram illustrating the mechanism of partial volume artifact with and off-axis image, the thick-dashed arrow represents the main beam, and the thin curved arrows represent the off-axis low energy beams. Images were obtained using a Philips Sparq machine and an L12-4 linear array transducer with a frequency range of 4 to 12 MHz and 37 mm footprint.

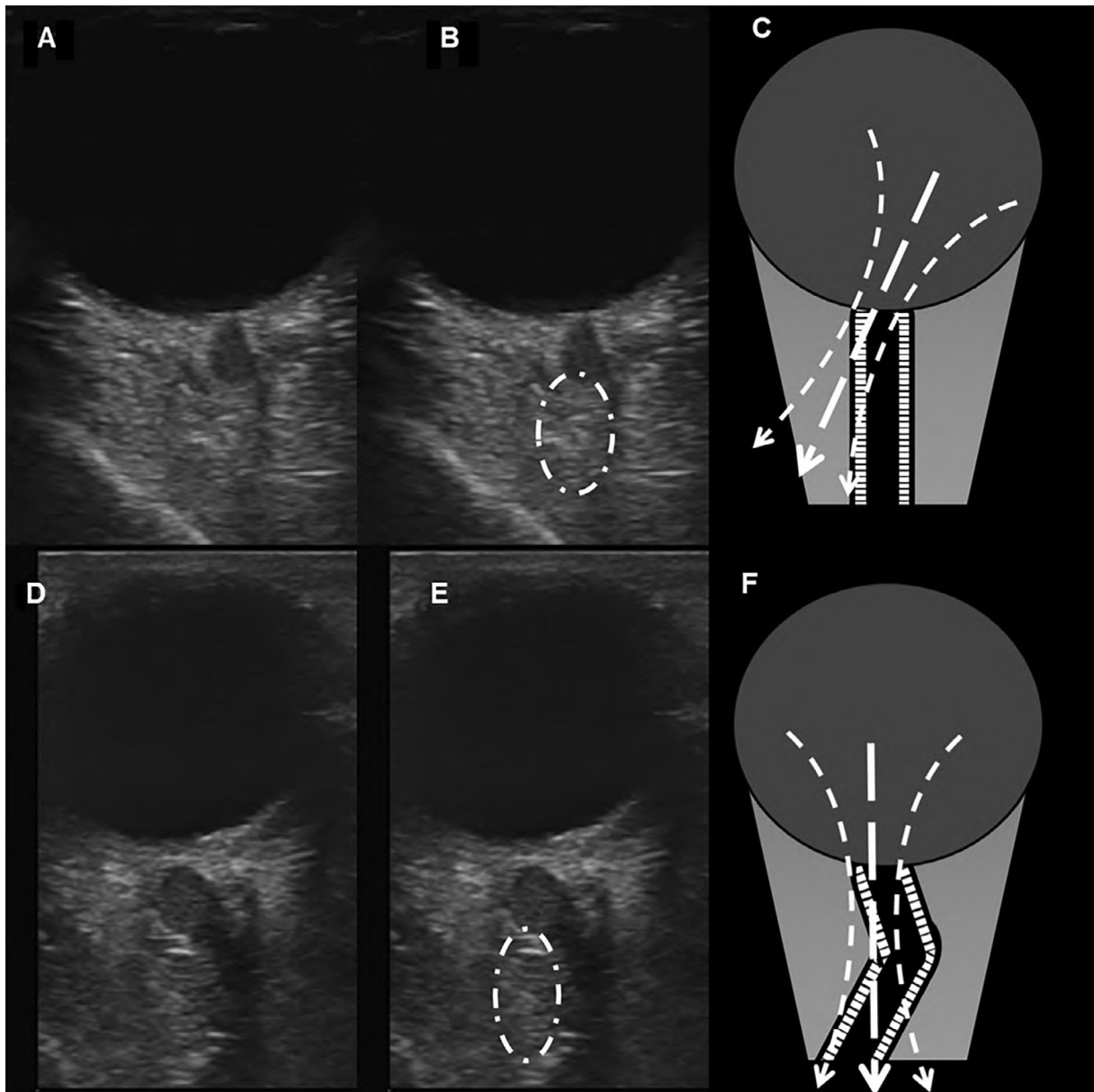
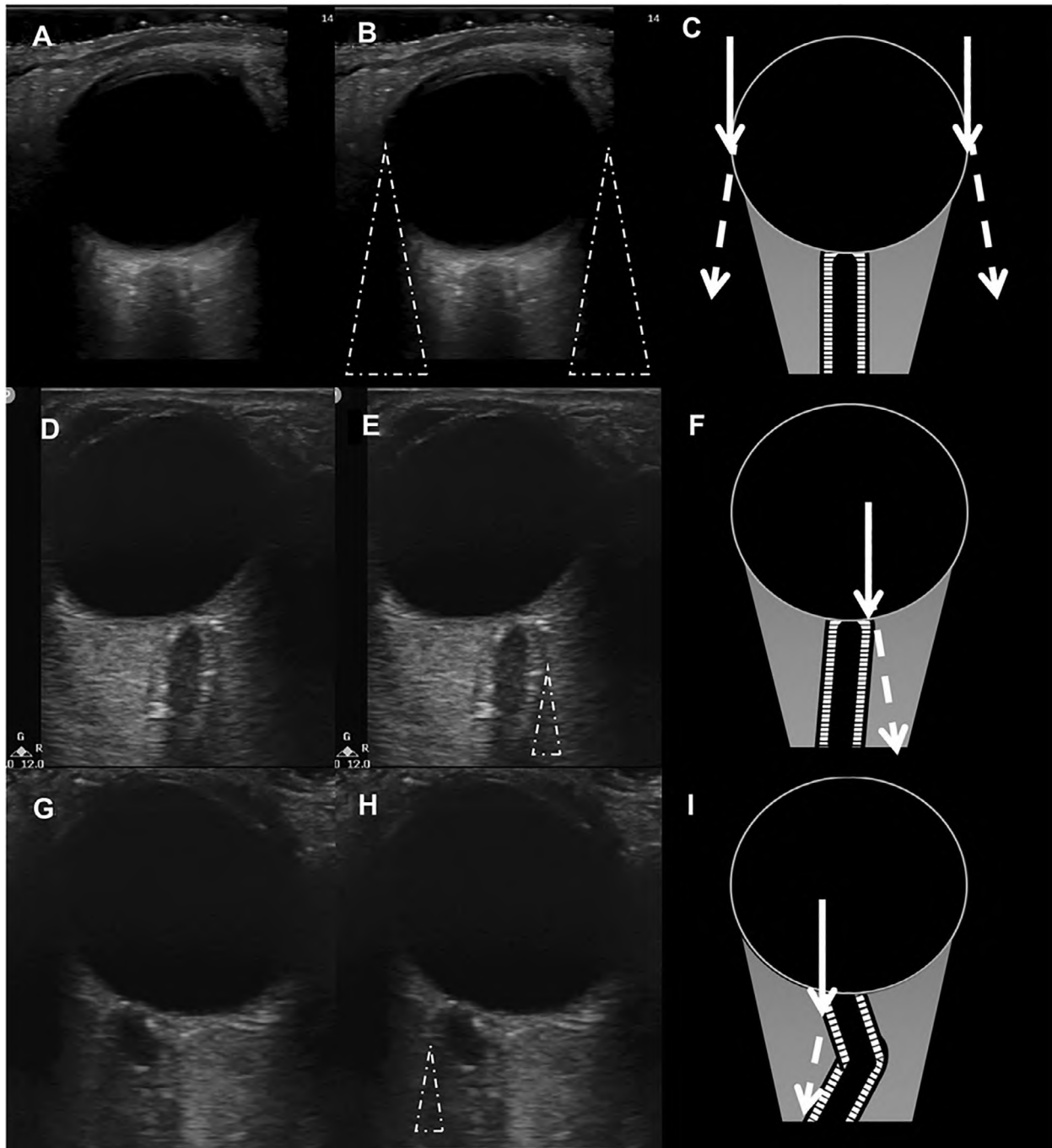


**Figure 15.** Different cases of refraction artifact. **A**, Demonstrates edge shadow artifact highlighter by the dashed triangles in **(B)**; **C**, Demonstrates the mechanism of edge shadow where the beam is refracted around the edges of the globe resulting in shadows. The solid arrow represents the original beam and dashed arrow the refracted beam; **D**, Demonstrates an edge shadow due to an off-axis imaging beam refracting around the edge of the ONS as represented by the dashed triangle in **(E)** and the arrows in panel **(F)**; **G**, Represents an edge shadow around the optic nerve head of a kinked optic nerve as represented by the dashed triangle in panel **H** and the arrows in panel **I**). Images were obtained using a Philips Sparq machine and an L12-4 linear array transducer with a frequency range of 4 to 12 MHz and 37 mm footprint.



adjusted to the right depth. As these adjustments are made, the operator should keep in mind that the ON diameter is  $\sim 3$  mm on average. Therefore, these adjustments need to be on sub-millimeter scale. This artifact may be unavoidable if the patient has a gaze deviation resulting in a kinked optic nerve. In these cases, focusing efforts on obtaining good anatomic differentiation at the standard 3 mm depth should be prioritized over not having artifacts. Gaze deviation is not the only cause of ON kinking and tortuosity, they may also be associated with elevated ICP and reversed upon ICP lowering.<sup>28,29</sup> Thus, ON tortuosity as noted on ultrasound imaging on sonography could potentially be an independent sign of elevated ICP, although this needs to be further studied. (Figure 14).

#### *Refraction Artifacts*

Refraction artifacts occur when the ultrasound beam arrives at a non-perpendicular angle at a tissue interface between two tissues with different ultrasound propagation speeds. This results in either convergence of the ultrasound beam if it is moving from higher to lower velocity or divergence if it is moving from lower to higher velocity.<sup>3,30</sup> Refraction artifacts can be encountered in three areas when imaging the ONS; namely when transitioning from the lens to vitreous fluid, as edge artifact around the edges of the globe, and during off-axis ONS imaging. Some authors suggest significant distortions if the ultrasound beam passes through the lens.<sup>31</sup> Considering that ultrasound speed is 1532 m/s in the vitreous and 1641 m/s in the lens,<sup>32</sup> this speed change may be enough to produce a meaningful image distortion. However, we have not been able to reproduce this artifact. There are no studies evaluating the magnitude of this effect in the context of ONSD measurement and formal study evaluating this issue is recommended. In the interim, expert consensus recommends carefully evaluating the image and excluding the lens if it is causing artifacts.<sup>5</sup> On the other hand, edge shadowing artifact and refraction around a kinked or off-axis nerve sheath are encountered more frequently and represented in Figure 15. These artifacts could be minimized by avoiding a non-perpendicular imaging axis relative to the structure generating the artifact.

## Conclusion

Specifying technical considerations during ultrasound imaging can reduce the variability in measurement<sup>11</sup> and expert consensus has been proposed to ensure reproducibility of measurements.<sup>33</sup> A recent effort standardized ONSD imaging and measurement using expert consensus<sup>5</sup> and while ONSD is gaining increased interest as a non-invasive ICP surrogate, several technical challenges may limit its use given the small size of the ONS and ultrasound imaging properties. It is therefore important to be aware of the effect of different ultrasound settings and proper alignment of the imaging axis with the nerve axis. Once the optimum settings and correct imaging axis alignment are achieved, it is important to recognize the normal appearance of the ONS and the artifacts that affect it. Thereafter, artifacts should be identified, followed by taking the necessary steps to mitigate their effect on ONSD assessment but understanding that the measurement may be performed even with the presence of artifacts if these artifacts do not obscure the portion of the ONSD used for measurement.

## Data Availability Statement

The data that support the findings of this study are available from the corresponding author upon reasonable request.

## References

1. Hirzallah MI, Choi HA. The monitoring of brain edema and intracranial hypertension. *J Neurocrit Care* 2016; 9:92–104. <https://doi.org/10.18700/jnc.160093>.
2. Hirzallah MI, Lochner P, Hafeez MU, et al. Quality assessment of optic nerve sheath diameter ultrasonography: scoping literature review and Delphi protocol. *J Neuroimaging* 2022; 32:808–824. <https://doi.org/10.1111/jon.13018>.
3. Prabhu SJ, Kanal K, Bhargava P, Vaidya S, Dighe MK. Ultrasound artifacts: classification, applied physics with illustrations, and imaging appearances. *Ultrasound Q* 2014; 30:145–157. <https://doi.org/10.1097/RUQ.0b013e3182a80d34>.

4. Quien MM, Saric M. Ultrasound imaging artifacts: how to recognize them and how to avoid them. *Echocardiography* 2018; 35: 1388–1401. <https://doi.org/10.1111/echo.14116>.
5. Hirzallah MI, Lochner P, Hafeez MU, et al. Optic nerve sheath diameter point-of-care ultrasonography quality criteria checklist: an international consensus statement on optic nerve sheath diameter imaging and measurement. *Crit Care Med* 2024; 52:1543–1556. <https://doi.org/10.1097/CCM.0000000000006345>.
6. U.S. Department of Health and Human Services Food and Drug Administration Center for Devices and Radiological Health. Marketing clearance of diagnostic ultrasound systems and transducers: guidance for industry and Food and Drug Administration staff. <https://www.fda.gov/media/71100/download>.
7. Pansell J, Bottai M, Bell M, Rudberg PC, Friman O, Cooray C. Which compartments of the optic nerve and its sheath are associated with intracranial pressure? An exploratory study. *J Neuroimaging* 2024; 34:572–580. <https://doi.org/10.1111/jon.13224>.
8. Pansell J, Bell M, Rudberg P, Friman O, Cooray C. Optic nerve sheath diameter in intracranial hypertension: measurement external or internal of the dura mater? *J Neuroimaging* 2023; 33:58–66. <https://doi.org/10.1111/jon.13062>.
9. Lawrence JP. Physics and instrumentation of ultrasound. *Crit Care Med* 2007; 35:S314–S322. <https://doi.org/10.1097/01.CCM.0000270241.33075.60>.
10. Gibbs V, Cole D, Sassano A. *Ultrasound Physics and Technology*. Philadelphia: Elsevier; 2009.
11. Gaarder M, Seierstad T. Measurements of carotid intima media thickness in non-invasive high-frequency ultrasound images: the effect of dynamic range setting. *Cardiovasc Ultrasound* 2015; 13:5. <https://doi.org/10.1186/1476-7120-13-5>.
12. Shriki J. Ultrasound physics. *Crit Care Clin* 2014; 30:1–24. <https://doi.org/10.1016/j.ccc.2013.08.004>.
13. Lieu D. Ultrasound physics and instrumentation for pathologists. *Arch Pathol Lab Med* 2010; 134:1541–1556. <https://doi.org/10.5858/2009-0730-RA.1>.
14. Grogan SP, Mount CA. *Ultrasound Physics and Instrumentation*. Treasure Island: StatPearls Publishing; 2024.
15. Lochner P, Behnke S, Fassbender K, et al. Simulation and experimental characterization of lateral imaging resolution of ultrasound systems and assessment of system suitability for acoustic optic nerve sheath diameter measurement. *J Neuroimaging* 2019; 29:34–41. <https://doi.org/10.1111/jon.12578>.
16. Steinborn M, Friedmann M, Makowski C, Hahn H, Hapfelmeier A, Juenger H. High resolution transbulbar sonography in children with suspicion of increased intracranial pressure. *Childs Nerv Syst* 2016; 32:655–660. <https://doi.org/10.1007/s00381-015-3001-2>.
17. Durouchoux A, Liguoro D, Sesay M, Le Petit L, Jecko V. Subarachnoid space of the optic nerve sheath and intracranial hypertension: a macroscopic, light and electron microscopic study. *Surg Radiol Anat* 2022; 44:759–766. <https://doi.org/10.1007/s00276-022-02948-1>.
18. Zaidman CM, Wu JS, Wilder S, Darras BT, Rutkove SB. Minimal training is required to reliably perform quantitative ultrasound of muscle. *Muscle Nerve* 2014; 50:124–128. <https://doi.org/10.1002/mus.24117>.
19. Steffel CN, Brown R, Korcarz CE, et al. Influence of ultrasound system and gain on grayscale median values. *J Ultrasound Med* 2019; 38:307–319. <https://doi.org/10.1002/jum.14690>.
20. Stevens RRF, Gommer ED, Aries MJH, et al. Optic nerve sheath diameter assessment by neurosonology: a review of methodologic discrepancies. *J Neuroimaging* 2021; 31:814–825. <https://doi.org/10.1111/jon.12906>.
21. Steinborn M, Fiegler J, Kraus V, et al. High resolution ultrasound and magnetic resonance imaging of the optic nerve and the optic nerve sheath: anatomic correlation and clinical importance. *Ultraschall Med* 2011; 32:608–613. <https://doi.org/10.1055/s-0029-1245822>.
22. Demer JL. Optic nerve sheath as a novel mechanical load on the globe in ocular duccion. *Invest Ophthalmol Vis Sci* 2016; 57:1826–1838. <https://doi.org/10.1167/iovs.15-18718>.
23. Saenz R, Cheng H, Prager TC, Frishman LJ, Tang RA. Use of A-scan ultrasound and optical coherence tomography to differentiate papilledema from pseudopapilledema. *Optom Vis Sci* 2017; 94: 1081–1089. <https://doi.org/10.1097/OPX.0000000000001148>.
24. Killer HE, Laeng HR, Flammer J, Groscurth P. Architecture of arachnoid trabeculae, pillars, and septa in the subarachnoid space of the human optic nerve: anatomy and clinical considerations. *Br J Ophthalmol* 2003; 87:777–781. <https://doi.org/10.1136/bjo.87.6.777>.
25. Aspide R, Bertolini G, Albini Riccioli L, Mazzatenta D, Palandri G, Biasucci DG. A proposal for a new protocol for sonographic assessment of the optic nerve sheath diameter: the CLOSED protocol. *Neurocrit Care* 2020; 32:327–332. <https://doi.org/10.1007/s12028-019-00853-x>.
26. Pansell J, Bell M, Rudberg P, Friman O, Cooray C. Optic nerve sheath diameter measurement by ultrasound: evaluation of a standardized protocol. *J Neuroimaging* 2022; 32:104–110. <https://doi.org/10.1111/jon.12936>.
27. Baad M, Lu ZF, Reiser I, Paushter D. Clinical significance of US artifacts. *RadioGraphics* 2017; 37:1408–1423. <https://doi.org/10.1148/rg.2017160175>.
28. Kwee RM, Kwee TC. Systematic review and meta-analysis of MRI signs for diagnosis of idiopathic intracranial hypertension. *Eur J Radiol* 2019; 116:106–115. <https://doi.org/10.1016/j.ejrad.2019.04.023>.
29. Hu R, Holbrook J, Newman NJ, et al. Cerebrospinal fluid pressure reduction results in dynamic changes in optic nerve angle on magnetic resonance imaging. *J Neuroophthalmol* 2019; 39:35–40. <https://doi.org/10.1097/WNO.0000000000000643>.

30. Scanlan KA. Sonographic artifacts and their origins. *AJR Am J Roentgenol* 1991; 156:1267–1272. <https://doi.org/10.2214/ajr.156.6.2028876>.
31. Sargsyan AE, Blaivas M, Geeraerts T, Karakitsos D. Ocular ultrasound in the intensive care unit. In: Lumb P, Karakitsos D (eds). *Critical Care Ultrasound*. Vol 1. 1st ed. Philadelphia: Saunders; 2014:45-50.
32. Atta HR. New applications in ultrasound technology. *Br J Ophthalmol* 1999; 83:1246–1249. <https://doi.org/10.1136/bjo.83.11.1246>.
33. Touboul P-J, Hennerici MG, Meairs S, et al. Mannheim carotid intima-media thickness and plaque consensus (2004–2006–2011). *Cerebrovasc Dis* 2012; 34:290–296. <https://doi.org/10.1159/000343145>.